2878–2886 *Nucleic Acids Research, 2006, Vol. 34, No. 10*
doi:10.1093/nar/gkl081

The naturally occurring N6-threonyl adenine in anticodon loop of *Schizosaccharomyces pombe* $tRNA_i$ causes formation of a unique U-turn motif

Eveline Lescrinier, Koen Nauwelaerts, Katia Zanier[1], Koen Poesen[1], Michael Sattler[1] and Piet Herdewijn*

Laboratory of Medicinal Chemistry, Rega Institute for Medical Research, BioMacs, K.U.Leuven, Minderbroedersstraat 10, B-3000 Leuven, Belgiumand and [1]EMBL, Structural & Computational Biology and Gene Expression, Meyerhofstrasse 1, D-69117 Heidelberg, Germany

Received December 23, 2005; Revised January 23, 2006; Accepted March 6, 2006

ABSTRACT

Modified nucleosides play an important role in structure and function of tRNA. We have determined the solution structure of the anticodon stem–loop (ASL) of initiator tRNA of *Schizosaccharomyces pombe*. The incorporation of *N6*-threonylcarbamoyladenosine at the position 3′ to the anticodon triplet (t^6A37) results in the formation of a U-turn motif and enhances stacking interactions within the loop and stem regions (i.e. between A35 and t^6A37) by bulging out U36. This conformation was not observed in a crystal structure of tRNAi including the same modification in its anticodon loop, nor in the solution structure of the unmodified ASL. A t^6A modification also occurs in the well studied anti-stem–loop of lys-$tRNA_{UUU}$. A comparison of this stem–loop with our structure demonstrates different effects of the modification depending on the loop sequence.

INTRODUCTION

A special methionine tRNA is used for the initiation of protein synthesis in all organisms. Two classes of methionine tRNA are found universally: the initiator tRNA ($tRNA_i$) that is used exclusively for translation initiation and elongator tRNA (met-$tRNA_e$) used for insertion of methionine into internal peptidic linkages (1,2).

Distinct mechanisms of translation initiation are used by prokaryotes and eukaryotes. In prokaryotes, the small ribosomal subunit (30S) forms an initiation complex with formylmethionine tRNA (fmet-$tRNA_i$) and a GTP binding protein called IF2 at certain AUG or AUG-cognate codons. In addition to IF2, also initiation factors IF3 and IF1 are required for initiation (3). Both of these factors stabilize the binding of fmet-$tRNA_i$·IF2 to the 30S subunit (4). IF3 contributes to the fidelity of initiation complexes that might form transiently at weak sites such as non-AUG codons (5). In cytoplasmic protein synthesis of eukaryotes, the small ribosomal subunit (40S) normally enters at the 5′ end of the mRNA and not at the AUG start-codon. The 40S subunit, carrying methionyl tRNA (met-$tRNA_i$), eIF2, GTP and other factors, then migrates through the 5′-untranslated region (5′-UTR) until it encounters the first AUG codon, which is recognized by base pairing with the anticodon met-$tRNA_i$. Selection of the start-codon is fixed when a large ribosomal subunit (60S) joins the paused 40S subunit (3).

In contrast with prokaryotic ribosomes, which often can also initiate at GUG or UUG, the eukaryote initiation mechanism does not allow an alternative codon to substitute for AUG *in vivo*. In yeast, the dominant role of every position of the anticodon in defining the initiator codon was demonstrated by changing the anticodon in met-$tRNA_i$ to 3′-UCC-5′ and showing that translation initiated exclusively at the first AGG codon in a test transcript (6). A strong codon–anticodon interaction is therefore prerequisite for correct translation initiation in the eukaryotic cytoplasm.

In all cytoplasmatic met-$tRNA_i$ of eukaryotes and plants a threonylcarbamoyl modification occurs at the 3′ site of the anticodon (t^6A37) whereas this nucleoside modification does not occur in fmet-$tRNA_i$ of prokaryotes, chloroplasts and archaeabacteria. It has been proposed that one of the roles of t^6A37 is to prevent mispairing between the first base of the codon and the third base of the anticodon (7).

*To whom correspondence should be addressed. Tel: +32 0 16 337387; Fax: +32 0 16 337340; Email: piet.herdewijn@rega.kuleuvan.ac.be

This idea was essentially based on the observation that Escherichia coli fmet-tRNA$_i$ recognizes not only the AUG initiator codon (~90%), but also GUG (~8%) and UUG (~1%), while yeast fmet-tRNA$_i$ with t^{6}A37 modification exclusively recognizes AUG *in vivo* (8,9). In thermodynamic and kinetic studies on yeast arg-tRNA it was shown that a t^{6}A37 modification has a stabilizing effect on U-A and U-G base pairs adjacent to the 5′-side of the modified nucleoside (10) *in vitro*. The solution structure showed that t^{6}A37 prevents the formation of a U33–A37 base pair that would force the anticodon loop towards an unfavorable conformation which would increase the entropic cost of tRNA binding (11). The crystal structure of modified lys-tRNA$_{UUU}$ anticodon stem–loops (ASL) bound to a 30S ribosomal subunit revealed a second way in which t^{6}A37 is favorable for codon–anticodon interaction: (12) the extended ring structure of t^{6}A37 enables cross-strand base-stacking of this modified nucleoside in the anticodon loop with A38 of tRNA and with A1, the base in the first position of the codon. This stacking arrangement helps to explain the observed increase in stability of the codon–anticodon interaction of the modified ASL versus that of the unmodified case.

RNA base pairing between the initiation codon and anticodon loop of initiator tRNA is essential but not sufficient for the selection of the 'correct' mRNA translational start-site by ribosomes. However, an anticodon:codon interaction between met-tRNA$_i$ and the first AUG, has a function in directing the ribosome to the eukaryotic initiator region as part of the scanning ribosome. The structure of the ASL of met-tRNA$_i$ is therefore of biological interest. The solution structure of the ASL of *E.coli* without modified nucleosides, was determined by Schweisguth *et al*. (13) A crystal structure of the entire eukaryotic tRNA$_i$ of *Saccharomyces cerevisiae* is available at the pdb databank (1YFG) but fails to reveal structural details of the ASL with its t^{6}A37 (14). We studied the ASL of *Schizosaccharomyces Pombe* (15), a unicellular eukaryote that is used as a model organism in molecular and cell biology, to determine the influence of the t^{6}A modification on the structure of the isolated ASL in eukaryotic tRNAi. t^{6}A is the only modified nucleoside present in the ASL of met-tRNAi in *S.pombe* (Scheme 1).

MATERIALS AND METHODS

NMR sample preparation

NMR sample conditions were 10 mM potassium phosphate (pH 7.4) with RNA concentrations of 0.6 mM. Samples were annealed prior to NMR experiments by briefly heating at 80°C and snap cooling on ice to promote hairpin formation. For spectra in D_2O, samples were lyophilized and dissolved in 100% D_2O.

NMR spectroscopy

Natural abundance [^{1}H,^{13}C]HSQC and NOESY spectra in D_2O were recorded on a Bruker DRX800 equipped with a 5 mm TXI HCN Z gradient cryoprobe (Centre for Biomolecular Magnetic Resonance, BMRZ, University, Frankfurt). Phosphorus spectra were obtained on a Bruker DRX600 spectrometer equipped with a broadband TBI probe. Other spectra are measured with our 'in house' Varian Unity 500 spectrometer using a 3 mm HCPzgrd probe. Unless stated differently, spectra were recorded at 22°C. Spectra were processed using the FELIX 97.00 software package (Biosym Technologies, San Diego, VA (Accelrys©)) running on a Silicon Graphics O2 R10000 workstation (IRIX version 6.3).

The 1D spectrum in H_2O was recorded using a jump-return pulse as the observation pulse (16). The 2D NOESY in H_2O (mixing time = 200 ms; at 5°C) was recorded using the WATERGATE water-suppression (17) with a sweep width of 10 000 Hz in both dimensions, 64 scans, 2048 data points in t2 and 512 FIDs in t1. The data were apodized with a shifted sine-bell square function in both dimensions and processed to a 2K × 1K matrix.

The 2D DQF-COSY (18), TOCSY (19) and NOESY (20) spectra in D_2O were recorded with a sweep width of 4200 Hz in both dimensions. The DQF-COSY spectrum consisted of

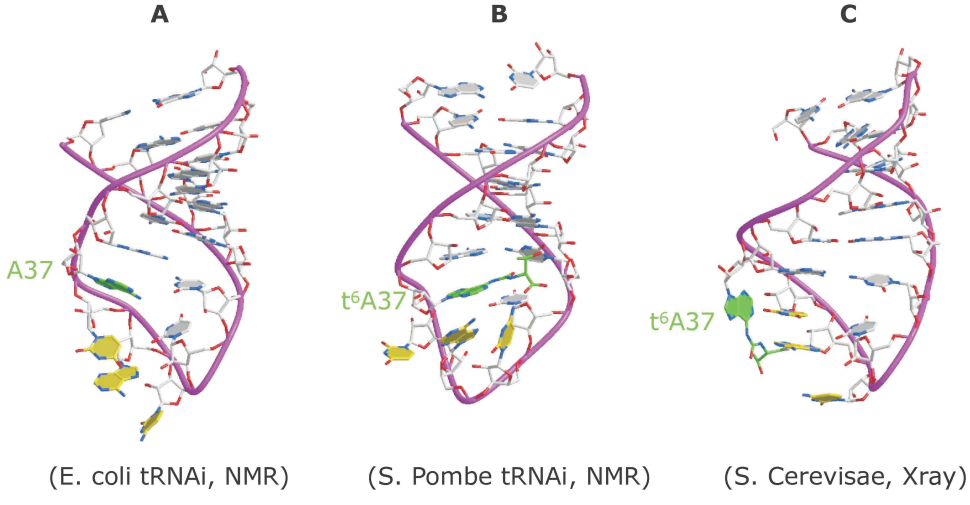

Figure 1. NMR structure of the unmodified ASL of *E.coli* tRNAi (residues 3 to 19) (13) (**A**), hairpin structures with the same loop-sequence including t6A modification at position 37 (green) (*S.pombe* tRNAi, structure closest to the average of refined NMR ensemble) (**B**) and X-ray crystallography (*S.cerevisiae* tRNAi residues 27 to 43) (14) (**C**). Ribbons are drawn through P atoms and nucleobases of the anticodon are depicted in yellow.

4096 data points in t2 and 512 increments in t1. The data were apodized with a shifted sine-bell square function in both dimensions and processed to a 4K × 1K matrix. Both ^{31}P-decoupled (on resonance, continuous decoupling) and ^{31}P-coupled spectra were recorded under the same conditions. For the TOCSY experiment, a clean DIPSI-2rc (21) was used, with a 90° pulse of 18.2 ms and a mixing tune of 65 ms. The total TOCSY mixing time was set to 64 ms. The spectrum was acquired with 32 scans, 2048 data points in t2 and 512 FIDs in t1. The data were apodized with a shifted sine-bell square function in both dimensions and processed to a 2K × 1K matrix. The NOESY experiments were acquired with mixing times of 50, 100, 150, 250 and 300 ms, 32 scans, 2048 data points in t2 and 512 increments in t1.

A ^{1}H-^{31}P HETCOR (22) spectrum was acquired with 256 scans, 2048 data points in the proton dimension, t2 and 256 increments in the phosphorus dimension, t1, over sweep widths of 4200 and 1600 Hz, respectively. The data were apodized with a shifted sine-bell square function in both dimensions and processed to a 2K × 1K matrix.

A natural abundance ^{1}H,^{13}C HSQC was recorded with sensitivity enhancement and gradient coherence selection optimized for selection of CH_2 groups (23) using 72 scans and 256/512 complex data points and 10 000/12 500 Hz spectral widths in t1 and t2, respectively.

Titration with $MgCl_2$ was monitored by 2D natural abundance [^{1}H,^{13}C]-HSQC spectra, 1D ^{1}H and ^{31}P spectra.

NMR derived restraints

Distance restraints were derived from NOESY spectra recorded with 50, 100 and 150 ms mixing times, using the FELIX 97.00 software (Accelrys©). Based on the build-up curves, inter-proton distances were calculated. An experimental error (±20%) was used on the calculated inter-proton distances. The calibration of NOE cross peak intensities was done against the H5–H6 cross peaks as an internal standard and resulted in 280 restraints.

Sugar puckers of the ribose's were inferred from the weak H1′ to H2′ scalar couplings. Residues C28–C32, A38–G42 and t^{6}A37 have H1′ to H2′ scalar couplings varying from 0 and 2 Hz and therefore were restrained to the N pucker conformation (24) [dihedral restraints applied: H1′-C1′-C2′-H2′ (99.2 ± 20°), H2′-C2′-C3′-C3′ (39.4 ± 20°), H3′-C3′-C4′-H4′ (−162.0 ± 20°)]. Residues U27, U33–U36 and A43 have larger H1′ to H2′ couplings (between 3 and 7 Hz). For this reason no restraints were applied on the sugar rings of these residues during the structure calculation.

The normal ^{31}P chemical shifts of most residues were used to restrain α and ζ torsion angles (0 ± 120°) (24). The α of residue U33 and ζ torsion angle of residue C32 were not restrained since U33:P showed a chemical shift deviating from the typical values of A-form RNA. Except for residue U36, nicely resolved H4′-P(n)-crosspeaks in the 2D ^{1}H-detected [^{1}H,^{31}P]HETCOR, allowed us to restrain the β and γ torsion angles to 180 ± 30° and 54 ± 30°, respectively (24). The α, β and γ torsion angles of residue U36 and ζ torsion angle of A35 were not restrained since they contain the phosphorus with a altered pattern in the 2D ^{1}H-detected [^{1}H,^{31}P]HETCOR.

The ε torsion angles were restrained (to 230° ± 70°) based on steric arguments (25).

Hydrogen bond restraints in the stem were applied as NOE-distance restraints (residues C27→G31 and C39→G43). No restraints on χ and no planarity restraints were used in the structure calculations.

Structure determination

All structure calculations were performed with X-PLOR-NIH V3.851 (26). The topallhdg.dna and parallhdg.dna files were adapted to include the modified residue using parameters obtained from *ab initio* calculations (27). In the topology file, a new t6A residue was introduced. The t6A residue was subsequently patched into the oligonucleotide sequence in a way comparable to the treatment of RNA and DNA in the standard X-PLOR program.

The torsion angle molecular dynamics protocol used was largely identical to that proposed for a DNA duplex (28). A set of 100 structures was generated by torsion angle molecular dynamics, starting from an extended strand and using NMR derived restraints.

After the torsion angle molecular dynamics round, the 39 structures had converged to very similar structures with similar total energies (189–381 kcal mol^{-1}) and no violations of the NOE and dihedral restraints Twenty lowest energy structures were used for further refinement during the 'gentle molecular dynamics' round.

The final refinement started with a 20 ps constant-temperature molecular dynamics simulation at 300 K (20 000 steps of 0.001 ps) and was followed by a 200-step conjugate gradient energy minimization of the average structure of the last 10 ps of the 20 ps simulation.

An analysis of the obtained 3D-structure with the computer programs X3DNA (29), was used to measure torsion angles and helix parameters. Finally, some visual representations of the molecule were obtained with Bobscript 2.4 (30).

RESULTS

Establishing optimal solution conditions

Sharp resonances were observed at pH 7.4 and 5.5, indicative that the structure is stable in a single predominant conformation in both conditions. Since pH 7.4 is closer to physiological conditions, we preferred to perform the structure determination at this pH.

Protonation of A38, which enhances the possibility of stable C32–A38^{+} base pair formation, was confirmed by the characteristic shift of the A38 C2 resonance to (C2:154 p.p.m.→148 p.p.m., H2:8.23 p.p.m.→8.33 p.p.m.) when lowering pH to 5.5 (31). However, there is no evidence that A38 is protonated at the physiological pH of 7.4.

Assigment of resonances

The ASL of *S.pombe* met-tRNAi was investigated by NMR using the chemically synthesized 17mer shown in Scheme 1. All aromatic, anomeric, H2′ and H3′ resonances could be assigned in the non-labeled sample starting from a standard anomeric to aromatic proton walk (32).

Non-exchangeable protons of residues in the stem region showed NMR spectral characteristics typical of an A-form

RNA duplex (24). In particular, nucleotides in the stem region displayed stronger intra-residue than inter-residue H8/H6–H1′ crosspeaks in NOESY spectra acquired with a 50 ms mixing time, as well as characteristic sequential H2′–H1′ and very strong sequential H2′–H8/H6 crosspeaks. In a typical A-form duplex RNA, sequential H2′–H8/H6 distances are <2.5 Å, intra-residue H1′–H8/H6 distances are in the range 3.5–4.0 Å and sequential H1′–H8/H6 distances are 1 Å longer. Except for the closing U27:A43 base pair, all ribonucleotides in the stem had small 3JH1′–H2′ as detected in DQF COSY experiments, thus intra-residue H1′–H2′ correlations were determined from NOESY spectra with short mixing times. In the loop, several NOE crosspeaks are observed that are not A-like: a correlation of U33:H1′ to A35:H8 and numerous crosspeaks between A35 and t^{6}A37. The sequential crosspeaks between atom pairs U36:H1′–t^{6}A37:H8 and U33:H1′–C34:H6 are absent but U33:H2′ and C34:H6 is clearly present. The typical NOE pattern between residues U33, C34 and A35 is a requisite feature of a U-turn 'fingerprint' (33). Important NOE-contacts were observed for threonine protons to sugar and base moieties in the loop region of the hairpin (Figure 2).

Assignment of imino–proton resonances was based on sequential imino–imino interactions and imino–aromatic contacts observed in a NOESY spectrum collected in 90% H_2O/10% D_2O (34). No signal was observed for the terminal U27:A43 base pair, which is attributed to fraying at the helix end. In addition to imino-signals from the stem, the H11 amide proton in the threonine moiety of t^{6}A was observed at 10.32 p.p.m. This amide proton shows NOE interactions with the purines H2, Hα and Hβ of the amino acid in t^{6}A37. Such pattern is expected for a side-chain coplanar to the parent base and results in the modified nucleobase adopting a tricyclic structure (11).

Phosphorus signals were assigned from a [^{31}P,^{1}H]Hetero-COSY experiment relating each phosphorus to intra-residue H5′/5″ and H3′ signals of the preceding residue. A downfield shift was observed for the C34:P signal which is typical in a U-turn motif (33). Carbon assignments are obtained from a [^{1}H,^{13}C] HSQC spectrum. This spectrum clearly shows that C5–H5 signals of C35, U33 and U36 are upfield shifted to random coil chemical shift values. Such a shift is indicative for absent ring current effects from 5′ neighbors induced by stacking interactions (35). A summary of the chemical shift assignments is listed in the Supplementary Data.

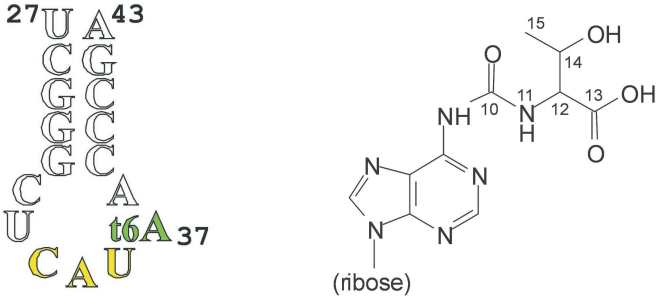

Scheme 1. Secondary structure of the studied ASL (left) and structure of the t^{6}A modification (right).

Structure determination

A total of 151 intra-residue and 108 inter-residue distance restraints were obtained for the 17 residue RNA oligomer. Most residues showed no H1′–H2′ crosspeaks in the 65 ms TOCSY spectrum, typical of N-type sugars (32). Intermediate TOCSY crosspeaks from H1′ to H2′ were observed for the fraying terminal residues (U27, A43) and 7 to 10 in the loop.

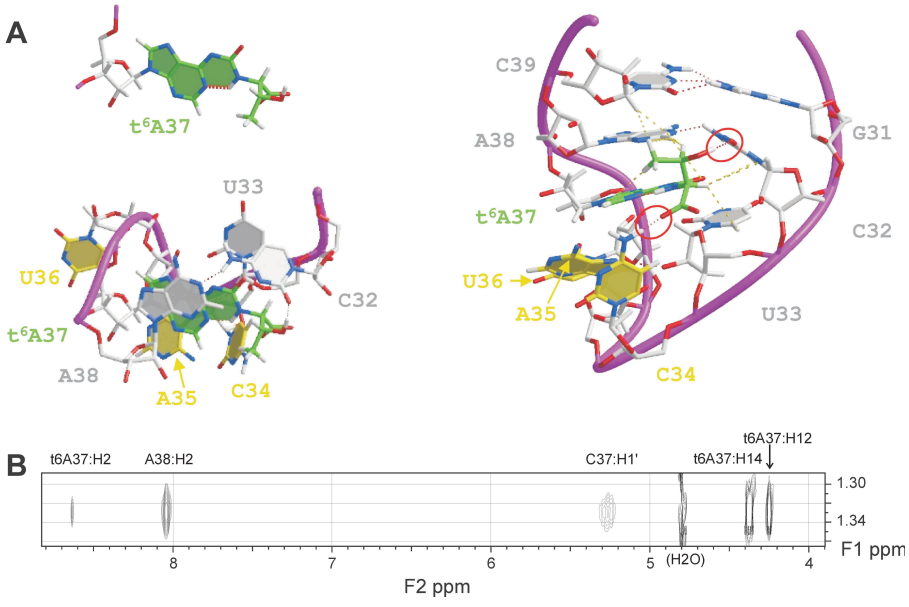

Figure 2. (**A**) Zoom of the tricyclic t6A residue (upper left). Side (right) and top view (lower left) of the loop region from the studied hairpin. Nucleobases of modified residue and the anticodon are depicted in green and yellow, respectively. A ribbon is drawn through P atoms. NOE distance restraints derived from NOE interactions of the threonine moiety in t^{6}A37, are indicated in yellow dashed lines. Red dashed lines connect atoms that are within hydrogen bonding distance. Red circles highlight hydrogen bonds of the threonine moiety in t^{6}A37 with other residues in the loop. (**B**) Strip of a noesy spectrum in D_2O (mix = 150 ms) at the resonance frequency of t6A37:H15, depicting some important NOEs in the loop region.

The sugar moieties of these residues were therefore not restrained during the structure calculations. Six negative distance constraints (33) with a lower bound of 4.0 Å, derived from absent crosspeaks in the measured NOESY spectra, were used during the first round of structure calculation. Hydrogen bonds in base pairs were treated as NOE distance restraints between the acceptor and donor heavy atoms.

The structure of the RNA hairpin was solved from 280 distance and 117 torsion angle restraints. Starting from an extended strand, a set of 100 structures was generated by torsion angle dynamics. Out of these 39 structures converged that had no NOE restraint violations >0.5 Å and no torsion angle restraint violations >5° (Table 1). These 39 accepted structures were subjected to refinement in a final round of energy minimization. The twenty lowest energy structures were selected for structural analysis (Table 1). Figure 3 shows the superposition of the 20 structures illustrating well-defined structures of the loop and stem region.

Binding of Mg^{2+} was monitored by NMR to detect specific binding sites in the loop region of the duplex. However, addition of Mg^{2+} did not induce significant chemical shift changes in ^{31}P or ^{1}H signals of the loop (Figure 4). Only slight chemical shift changes of loop signals occurred in the ^{1}H spectrum at increasing Mg^{2+} concentration from 0 to 1 mM. Notably, ^{31}P signals characteristic for the U-turn (U33:P) and the bulged-out U36 in the anticodon loop (A35 and U36:P), did not shift significantly when Mg^{2+} was added to the sample. These results indicate that there is no major conformational change within the anticodon loop that could be caused by specific Mg^{2+} binding. Absence of tight Mg^{2+} binding in the studied ASL is in agreement with the very weak Mg^{2+} induced cleavage of this loop observed for Yeast met-tRNAi that was attributed to low affinity of metal ions or a less favorable structure of this loop for efficient cleavage (36).

DISCUSSION

Structure of the ASL of *S.pombe*

As expected for double stranded RNA, the stem-region adopts a typical A-form structure. There is no direct evidence that A38 is protonated (at pH 7.4) and involved in an A38+.C32 pair. However, much indirect evidence seems to point to it and resulted in a structure that contains a A38:C32 base pair. The NMR data indicate that the stem is extended beyond the G31·C39 pair and that A-form stacking continues on the 5′ side and as well as on 3' side. Although no assumptions or explicit hydrogen bond restraints were introduced to force the A38–C32 mismatch (Figure 2, left), in the 39 refined structures A38:N1 and C32:N4 are within hydrogen bonding distance (<3.0 Å) to form an A:C N1-amino base pair (37) (Table 2).

The loop portion was very well-defined by the NMR restraints of the threonine moiety in t^6A37 (Figure 3) and 11 NOE interactions of base protons in A35. Structure calculations therefore resulted in a highly defined structure that shows t^6A37:O13A and t^6A37:OH14 within hydrogen bonding distance of C34:N4 and C32:O2, respectively (<3.0 Å) (Figure 2, right). As in GNRA tetraloops, whose NMR structures show low pairwise RMSD (33), a network of heterogeneous hydrogen bonds and extensive base stacking in the loop contribute to the highly defined loop-structure.

The residue U36 is completely bulged out while A35 is stacking on t^6A37. This rather unexpected structural feature is supported by the observed NOE-contacts and the upfield chemical shift of U36:H5 that is in agreement with absent stacking interactions of a bulged out pyrimidine while the A35:H8 signal is in the region typical for an A-type helix (35). As depicted in Figure 2 (left), the tricyclic t^6A37 nucleobase (green) is stacked between A35 (yellow) and A38 (grey) while U36 is completely bulged out. The helical twist of A35 relative to t^6A37 in the structure closest to the average of all refined structures is 33.79° (Curves: Lavery and Sklenar) (38), a value that is comparable to the 31.4 Å found in A-type RNA (25). The bulged out U36 residue exposes its nucleobase into the solvent, making it available for possible tertiary interactions. That U36 would have a natural tendency to bulge out was suggested in literature reports since it is an unpaired uridine (39) and it is the n + 3 residue in a U-turn (below). Conflicting structures of the conserved GUAAUA

Table 1. Refinement statistics for the final set of 20 structures and overview of the NMR constraints used during structure calculation

Total energy (kcal mol^{-1})	418.5 ± 3.6
NOE violations (>0.5 Å)	0
NOE constraints	274 (280)
inter-residue	108
intra-residue	151
base pairing	15
non-noe	6
Dihedral violations (>5°)	1 ± 1
Torsion angle constraints	117
RMSD from distance restraints (Å)	0.059 ± 0.001
RMSD from dihedral restraints (°)	0.837 ± 0.038
RMSD in Å omitting the closing base pair (U27–A43)	0.09–00.24

Non-noe constraints were used during the torsion angle dynamics but omitted in the refinement stage Reported RMSD is the average of all heavy atoms in a refined structure relative to the average of the 20 selected structures (0.09 Å = structure closest to the average of refined structures).

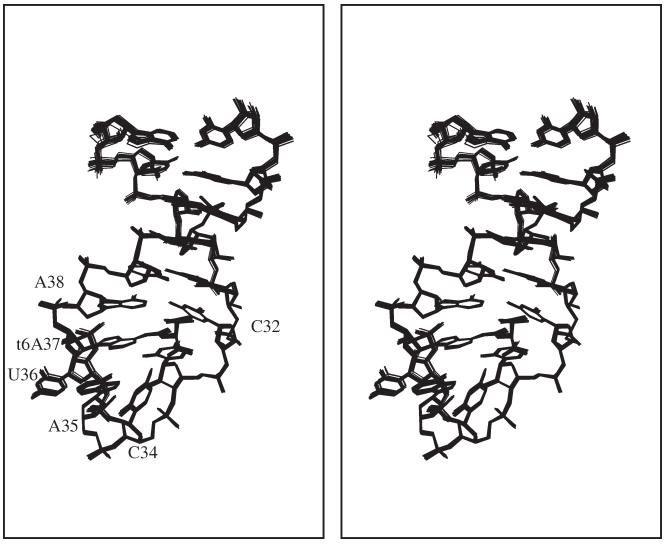

Figure 3. Stereo overlay of the 20 lowest energy structures fitted to all residues except those in the closing base pair (U27–A43).

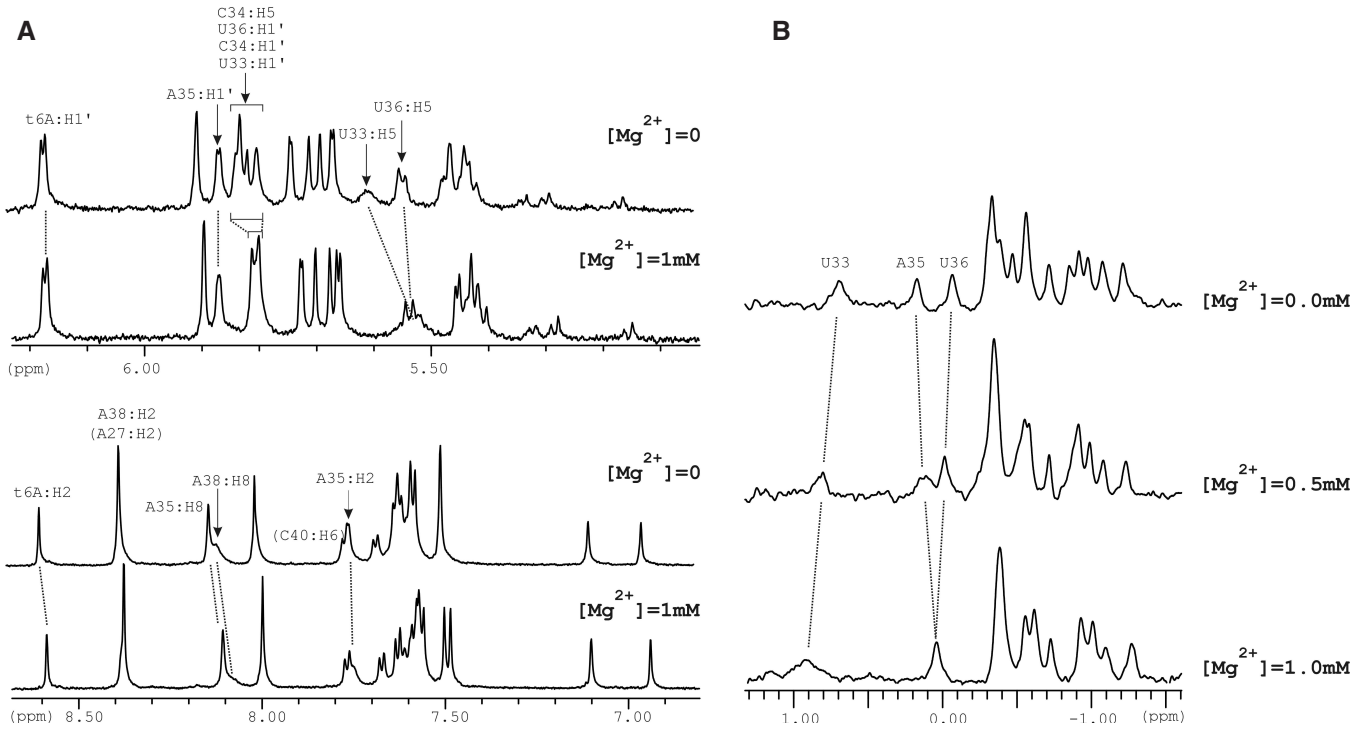

Figure 4. 1D ^{1}H (**A**) and ^{31}P (**B**) spectra at different Mg^{2+} concentrations. H5 and H1′ signals close to the water are influenced by the applied water-suppression (watergate). Signals that are significant for the loop structure are indicated.

hexaloop in ribosomal RNA are reported in literature. In the hairpin structure determined by Huang *et al*. (40) the consecutive residues UAA adopt a U-turn stacked on a non-canonical GA base pair while the last uridine in the loop is bulged out. However, Fountain *et al*. (41) describes the structure of this loop with two non-canonical base pairs (GA and UU) and two unpaired adenines. It is possible that the increased concentration of salts used by these authors induced the conformational change in their loop: the structure of Huang *et al*. (40) was determined from a 1.5 mM hairpin sample at pH 6 (5 mM sodium phosphate buffer) containing 30 mM NaCl and 0.04 mM EDTA while Fountain *et al*. (41) used a 1.8 mM oligomer sample at pH 7 (10 mM sodium phosphate buffer) with 100 mM NaCl and 0.5 mM EDTA.

A slightly modification of a 'classical' U-turn occurs starting from residue U33 (Scheme 2). The U-turn is an RNA structural motif that was first identified in the crystal structure of the yeast Phe-tRNA anticodon loop (42) and is now recognized as a basic architectural unit of many RNA molecules. This RNA motif reverses the direction of the phosphate backbone, frequently 3′ to a uridine nucleotide. The turn is achieved by adoption of the nonstandard *trans* conformation of the α torsion angle 3′ to U33. It is stabilized by stacking interactions of U33 with C32 and between A35 and t^6A37. The hydrogen bond between U33:H3 and the phosphate group of U36, known to stabilize a U-turn (25), are not present in the studied ASL due to the altered position of U36. However atoms U33:O2′ and A35:N7 are within hydrogen bonding distance (2.68 Å) as expected in a U-turn (25). As in a 'classical' U-turn, the Watson–Crick faces of both nucleobases following the turning phosphate are exposed towards the solvent and prone to interact with cognate bases of mRNA.

Table 2. Atom pairs in the loop of the calculated structures that are within hydrogen bonding distance

H-donor	H-acceptor	distance
t^6A37:OH14	C32:O2	1.35 (0.02)
C34:N4	t^6A37:O13[a]	2.47 (0.15)
U33:O2′	A35:N7	2.89 (0.07)
C32:N4	A38:N1	2.64 (0.04)

Distances and their RMSD in the 20 selected structures are listed in Å.
[a]O13A or O13B, whichever is turned towards C34:N4.

Comparison with relevant tRNA structures

Based on the RMSD difference of modified and unmodified structures, introduction of a t^6A modification restricts the conformational space of the anticodon loop (unmodified: 0.3–0.9 Å, modified: 0.09–0.23 Å). The loop structure we determined is not only better defined, but also differs significantly from its unmodified relative depicted in the left panel of Figure 1 (13). The five Watson–Crick base pairs and a non-canonical C32.A38 base pair in the stem of both structures are in the standard A-form of helical RNA. The t^6A37 adjacent to the anticodon adopts the form of a tricyclic nucleoside with an intra-residue hydrogen-bond and alters base stacking on the 3′-side of the anticodon loop. U36 of the anticodon is significantly displaced by the presence of t^6A and allows A35 to stack on t^6A37. Both modified and unmodified loops contain a U-turn motif, formed by residues U33, C34 and A35. However the residue stacking on the 3′ side of the U-turn differs: in the unmodified loop this stacking occurs with U36 while bulging out of U36 by the t^6A modification induces stacking of A35 on t^6A37, which in turn stacks on the adjacent stem. Apparently,

the modification structures the loop by extra hydrogen bonds of the threonyl side chain with several loop-residues and increased stacking on the stem at its 3′ side. All three nucleobases of the anticodon in the modified loop have their Watson-Crick binding faces exposed to the solvent. In the unmodified hairpin, the loop also presents three anticodon bases for codon-binding, although their positions are not as well-defined and stacking between U36 and A37 is absent.

The ASL in the crystal structure of *S.cerevisiae* met-tRNAi (1YFG, right panel of Figure 1) is significantly different from the solution structure we describe here: t^6A37 is bulged out, a U-turn is formed by U33-C34-A35 and all three anticodon nucleobases (C34,A35,U36) are stacked on top op of A38, extending the 5′ end of the stem. However, according to the authors, the anticodon loop in their crystal structure is not well enough defined to discuss confidently the implications of its structure in initiation of translation. Moreover, the anticodon in this structure is involved in lattice contacts, which may have imposed a stereochemistry that may not exist in solution (14).

As in the structure we determined, the t^6A modification in the ASL of lys-tRNA$_{UUU}$ (1FEQ, Figure 5B) is t^6A stacking on 5′ side of the stem and has a tricyclic nature by an intraresidue hydrogen bond of the threonyl side chain with N7 of adenine (11). Durant *et al*. (43) also studied this loop-modification and report that t^6A decreases anticodon stacking in the loop by promoting U36 bulging. However, also in their structure U36 is not completely bulged out as what we observe in the modified initiator tRNA-loop. The A35-t^6A37 stacking in our structure clearly contributes to stabilization of a structure with bulged out U36. In the unmodified ASL of in lys-tRNA$_{UUU}$ (2BZ1, Figure 5A), the loop is rather dynamic with only weak stacking between U35–U36 and no NOEs that would indicate base stacking between U34 and U35 (44). The poor stacking was attributed to the loop sequence composed of consecutive uridines that are known to have weak stacking interactions (25). In this unmodified loop, non-specific Mg2+ (15 mM) apparently promotes U36-A37-A38 stacking. A high resolution NMR structure is also available for the hyper-modified ASL of *E.coli* lys-tRNA$_{UUU}$ with t^6A and 5-methylaminomethyl-,2-thiouridine (mnm^{5}s^{2}U34) in the loop section (Figure 5D) (45). The ^{31}P spectrum of this loop has 33p34 shifted significantly downfield, consistent with U-turn geometry where nucleobases of the 3′ side of the loop starting at position 34 are stacked in an A-form geometry with the double stranded stem beginning at residue 39. Apparently, the presence of only t^6A in 1FEQ does not induce this U-turn and U34 in lys-tRNA$_{UUU}$ is displaced in the loop, away from other anticodon uridines and is not exposing its Watson–Crick face to the solvent. The hypermodification induces formation of a nearly canonical tRNA anticodon loop; however, the loop

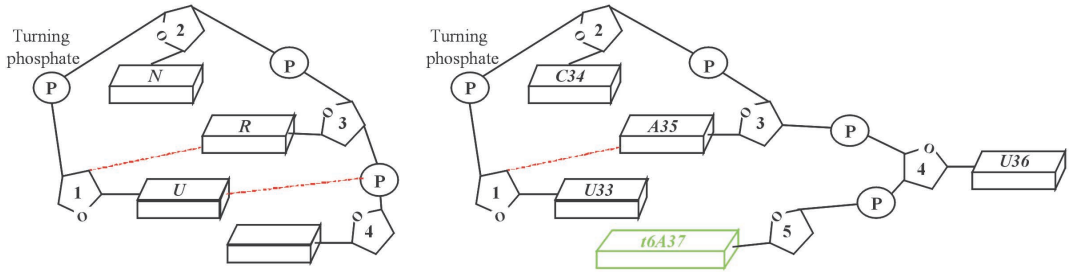

Scheme 2. Representation of a 'classical' U-turn (left) (25) and the U-turn in the ASL of *S.pombe* met-tRNAi (right) on left and right panels, respectively. R represents a purine and N a purine or pyrimidine nucleobase. Stabilizing hydrogen bonding interactions of the U-imino with 5′ phosphate following the UNR sequence and of 2′ hydroxyl of U with R:N7 are indicated in red dashed lines. Atoms U33:O2' and A35:N7 that are within hydrogen bonding distance are also connected by a red dashed line.

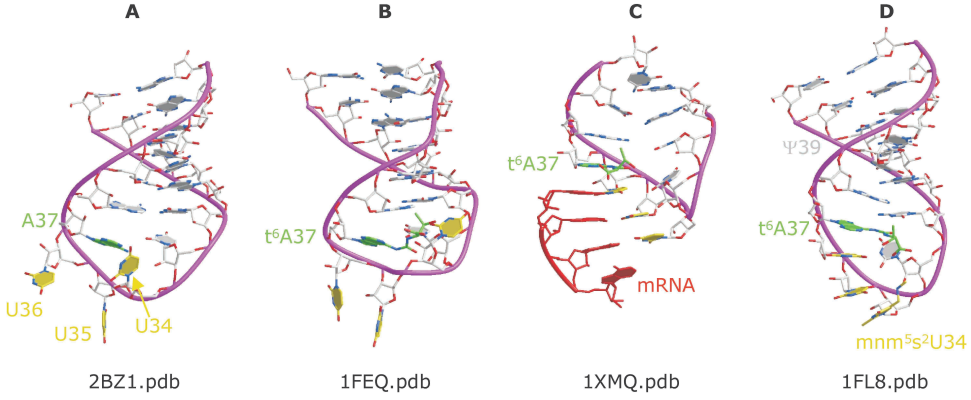

Figure 5. (**A**) 2BZ1: the unmodified ASL of Lys-tRNA$_{UUU}$) (43), (**B**) 1FEQ: hairpin structure with the same sequence including t^6A modification at position 37 (11), (**C**) 1×MQ: the same ASL as in 1FEQ and cognate mRNA (red) as they occur in the A-site of the crystal structure bound to a 30S ribosomal subunit (12) and (**D**) 1FL8 : hypermodified ASL with same nucleoside sequence including mnm^{5}s^{2}U34, t^6A37 and Ψ39 (44). The right structure is determined by christallography, others are determined by NMR spectroscopy. Ribbons are drawn through P atoms and nucleobases of the UUU-anticodon are depicted in yellow.

uridine riboses still interconvert between 2′ endo and 3′ endo conformations because of weak uridine stacking. The crystal structure of human lys-$tRNA_{UUU}$ that has mcm^5s^5U34 and ms^2t^6A37 modifications in its anticodon loop, demonstrates that when anticodon residues are base paired their ribose conformation becomes 100% 3′ endo within the context of an A-type RNA duplex (46).

However, the presence of the typical 'tRNA-like' structure with three anticodon nucleotides positioned to bind the cognate codon to form an A-type double helical RNA complex with mRNA (Figure 5C) is not required for protein synthesis, since presence of t^6A37 in ASL of lys-$tRNA_{UUU}$ enables to bind AAA in the A-site of the ribosome (12), a feature that is absent for the unmodified lys-tRNA stem–loop (47). Combination of modifications, t^6A37 and mnm^5s^2U34, in ASL of lys-$tRNA_{UUU}$ enables binding to AAA and AAG codons in the ribosome (12). Such a wobbling does not occur with met-$tRNA_i$ since it only initiates translation at an AUG start-codon *in vivo*.

Critically important in lys-$tRNA_{UUU}$ is that the base modification negates the formation of an intraloop U33.A37 base pair that as is observed in the unmodified ASL. This therefore reduces the energetic cost for base exposure during codon–anticodon binding. In the structure of the *E.coli* tRNAi residues A37 and U33 are coplanar but no base pairing occurs between them according to the measured distances. The presence of a tricylic t^6A in our structure slightly displaces U33 further away from its position in the unmodified loop, negating the possibility of an U33.t^6A37 base pair in the loop.

CONCLUSION

The anticodon loop is a region with high conformational diversity dependence on sequence, the presence of modified nucleosides and its environment. The t^6A modification of tRNA in the ASL, 3′ adjacent to the anticodon, is known to facilitate codon recognition and negate translational frame shifting. The presence of t^6A37 in the ASL of met-$tRNA_i$ reduces its flexibility and causes rearrangements of the loop structure that adopts a type of U-turn that was not observed previously. Structural changes caused by the presence of the t^6A modification do not result in the typical 'tRNA-like' structure with three anticodon nucleotides positioned to bind the cognate codon to form an A-type double helical RNA complex with mRNA. However, previous studies on the ASL of $tRNA_{UUU}$ demonstrated that such a highly pre-organized structure of the anticodon loop is not required for codon-binding, but induces wobbling at the third codon position. Such a wobbling is not desired for met-$tRNA_i$, since it would cause inaccuracy in the initiation of protein synthesis.

While the unmodified anticodon loop can be considered as a point of structural dynamics in the prokaryotic met-$tRNA_i$ molecule, the threonyl side chain of t^6A37 in eukaryotic met-$tRNA_i$ creates a tricyclic nature of t^6A that enhances stacking interactions of the loop and stem region. Additional hydrogen bonds of this threonyl side chain with different nucleosides in the loop also increase loop stability. Because the threonyl moiety must accommodate within the loop, U33 is slightly shifted and U36 is completely bulged out. The latter enables efficient A35 to t^6A37 stacking following a U-turn. Here, we demonstrated that a unique U-turn motif in a hairpin loop can be obtained by introducing one modified nucleoside (t^6A). When evaluating the structure of the ASL of tRNAi of *S.pombe*, the modified t^6A37 might help in presenting decoding bases outside the loop structure which is not the case for the unmodified loop and cannot be concluded from the X-ray structure. Whether the bulged U36 has a functional role in initiating the recognition process leading to eukaryote translation remains a subject for further studies.

ACKNOWLEDGEMENTS

The authors thank Brian Sproat for the synthesis of the oligomers and Ingrid Luyten for initial experiments. E.L. and K.N. are Research fellows of the Fund for Scientific Research—Flanders (Belgium). The authors thank the European NMR Large Scale Facility in Frankfurt for access to the 800 MHz spectrometer. The refined coordinates of the twenty structures closest to the average are deposited in the Brookhaven Protein Data Bank (2G1G.pdb) together with the measured chemical shifts and experimental restraints. Funding to pay the Open Access publication charges for this article was provided by K.U.Leuven.

Conflict of interest statement. None declared.

REFERENCES

1. Kozak,M. (1983) Comparison of initiation of protein synthesis in prokaryotes, eukaryotes and organelles. *Microbiol. Rev.*, **47**, 1–45.
2. Smith,A.E. and Marcker,K.A. (1970) Cytoplasmatic methionine transfer RNAs from eukaryotes. *Nature*, **226**, 607–610.
3. Kozak,M. (1999) Initiation of translation in prokaryotes and eukaryotes. *Gene*, **234**, 167–208.
4. Maitra,U., Stringer,E.A. and Chaudhuri,A. (1982) Initiation factors in protein synthesis. *Ann. Rev. Biochem.*, **51**, 869–900.
5. Meinnel,T., Sacerdot,C., Graffe,M., Blanquet,S. and Springer,M. (1999) Discrimitation by—initiation factor IF3 against initiation on non-canonical codons relies on complementarity rules. *J. Mol. Biol.*, **390**, 825–837.
6. Cigan,A.M., Feng,L. and Donahue,T.F. (1988) met-tRNAi functions in directing the scanning ribosome to the start site of translation. *Science*, **242**, 93–97.
7. Dube,S., K, Marcker,K.A., Clark,B.F.C. and Cory,S. (1968) Nucleotide sequence of N-formyl-methionyl-transfer RNA. *Nature*, **218**, 232–233.
8. Baralle,F.E. and Brownlee,G.G. (1978) AUG is the only recognisable signal sequence in the 5′ non-coding regions of eukaryotic mRNA. *Nature*, **274**, 84–87.
9. Schneider,T.D., Stormo,G.D., Gold,L. and Ehrenfeucht,A. (1986) Information content of binding sites on nucleotide sequences. *J. Mol. Biol.*, **188**, 415–431.
10. Weissenbach,J. and Grosjean,H. (1981) Effect of threonylcarbamoyl modification (t6A) in yeast tRNAArgIII on codon–anticodon and anticodon–anticodon interactions. *Eur. J. Biochem.*, **116**, 207–213.
11. Stuart,J.W., Gdaniec,Z., Guenther,R., Marszalek,M., Sochacka,E., Malkiewicz,A. and Agris,P.F. (2000) Functional anticodon architecture of human tRNAlys3 includes disruption of intraloop hydrogen bonding by the naturally occcurring amino acid modification ^{t6}A37. *Biochemistry*, **39**, 13396–13404.
12. Murphy,F.V., Ramakirshnan,V., Malkeiwicz,A. and Agris,P.F. (2004) The role of modifications in codon discrimination by lys-$tRNA_{UUU}$. *Nature Struct. Biol.*, **111**, 1186–1191.
13. Schweisguth,D.C. and Moore,P.B. (1997) On the conformation of the anticodon loops of initiator and elongator methionine tRNAs. *J. Mol. Biol.*, **267**, 505–519.

14. Basavappa,R. and Sigler,P.B. (1991) The 3 A crystal structure of yeast initiator tRNA: functional implications in initiator/elongator discrimination. *EMBO J.*, **10**, 3105–3111.
15. Keith,G., Heitzler,J., el Adlouni,C., Glasser,A.L., Fix,C., Desgres,J. and Dirheimer,G. (1993) The primary structure of cytoplasmic initiator tRNA(Met) from *Schizosaccharomyces pombe*. *Nucleic Acids Res.*, **21**, 2949.
16. Plateau,P. and Gueron,M. (1982) Exchangeable proton NMR without base-line distortion, using new strong-pulse sequences. *J. Am. Chem. Soc.*, **104**, 7310–7311.
17. Piotto,M., Saudek,V. and Sklenar,V. (1992) Gradient-tailored excitation for single-quantum NMR-spectroscopy of aqueous-solutions. *J. Biomol. NMR*, **2**, 661–665.
18. Rance,M., Sorensen,O.W., Bodenhausen,G., Wagner,G., Ernst,R.R. and Wuthrich,K. (1983) Improved spectral resolution in cosy H-1-NMR spectra of proteins via double quantum filtering. *Biochem. Biophys. Res. Commun.*, **117**, 479–485.
19. Bax,A. and Davis,D.G. (1985) Mlev-17-based two-dimensional homonuclear magnetization transfer spectroscopy. *J. Magn. Reson.*, **65**, 355–360.
20. Jeener,J., Meier,B.H., Bachmann,P. and Ernst,R.R. (1979) Investigation of exchange processes by 2-dimensional NMR-spectroscopy. *J. Chem. Phys.*, **71**, 4546–4553.
21. Cavanagh,J. and Rance,M. (1992) Suppression of cross relaxation effects in TOCSY spectra via a modified DIPSI-2 mixing sequence. *J. Magn. Reson.*, **96**, 670–678.
22. Sklenar,V., Miyashiro,H., Zon,G., Miles,H.T. and Bax,A. (1986) Assignment of the P-31 and H-1 resonances in oligonucleotides by two-dimensional NMR-spectroscopy. *Febs Lett.*, **208**, 94–98.
23. Schleucher,J., Schwendinger,M., Sattler,M., Schmidt,P., Schedletzky,O., Glaser,S.J., Sorensen,O.W. and Griesinger,C. (1994) A general enhancement scheme in heteronuclear multidimensional NMR employing pulsed field gradients. *J. Biomol. NMR*, **4**, 301–306.
24. Wijmenga,S. and van Buuren,B.N.M. (1998) The use of NMR methods for conformational studies of nucleic acids. *Prog. Nucl. Mag. Res. Sp.*, **32**, 287–387.
25. Saenger,W. (1984) Principles of nucleic acid structure. In Cantor,C.R. (ed.), *Springer Advanced Texts in Chemistry*. Springer Verlag, New York.
26. Schwieters,C.D., Kuszewski,J.J., Tjandra,N. and Clore,G.M. (2003) The Xplor-NIH NMR molecular structure determination package. *J. Magn. Reson.*, **160**, 65–73.
27. Schmidt,M.W., Baldridge,K.K., Boatz,J.A., Elbert,S.T., Gordon,M.S., Jensen,J.H., Koseki,S., Matsunaga,N., Nguyen,K.A., Su,S., Windus,T.L., Dupuis,M. and Montgomery,J.A.,Jr (1993) The general atomic and molecular electronic structure system. *J. Comput. Chem.*, **14**, 1347–1363.
28. Stein,E.G., Rice,L.M. and Brunger,A.T. (1997) Torsion-angle molecular dynamics as a new efficient tool for NMR structure calculation. *J. Magn. Reson.*, **124**, 154–164.
29. Lu,X.J., Shakked,Z. and Olson,W.K. (2000) A-form conformational motifs in ligand-bound DNA structures. *J. Mol. Biol.*, **300**, 819–840.
30. Esnouf,R.M. (1997) An extensively modified version of molscript that includes generally enhanced colouring capabilities. *J. Mol. Graph. Model.*, **15**, 132–134.
31. Legault,P. and Pardi,A. (1994) *In situ* probing of adenine protonation in RNA by ^{13}C NMR. *J. Am. Chem. Soc.*, **116**, 8390–8391.
32. Wijmenga,S.S., Mooren,M.W. and Hilbers,C.W. (1993) NMR of nucleic acids; from spectrum to structure. In Roberts,G.C.K. (ed.) *NMR of Macromolecules. A Practical Approach.*. Oxford University Press, NY, pp. 217–288.
33. Jucker,F.M., Heus,H.A., Yip,P.F., Moors,E.H. and Pardi,A. (1996) A network of heterogeneous hydrogen bonds in GNRA tetraloops. *J. Mol. Biol.*, **264**, 968–980.
34. Wüthrich,K. (1986) *NMR of Proteins and Nucleic Acids*. John Wiley & Sons Inc., New York, NY.
35. Cromsigt,J.A.M.T.C., Hilbers,C.W. and Wijmenga,S.S. (2001) Prediction of proton chemical shifts in RNA. Their use in structure refinement and validation. *J. Biomol. NMR*, **21**, 11–29.
36. Ciesiolka,J., Wresinski,J., Gornicki,P., Podkowinski,J. and Krzyzosiak,W.J. (1989) Analysis of magnesium, europium and lead binding sites in methionine initiator and elongator tRNA's by specific metal-ion-induced cleavages. *Eur. J. Biochem.*, **186**, 71–77.
37. Nagaswamy,U., Voss,N., Zhang,Z. and Fox,G.E. (2000) Database of non-canonical base pairs found in known RNA structures. *Nucleic Acids Res.*, **28**, 375–376.
38. Lavery,R. and Sklenar,H. (1989) Defining the structure of irregular nucleic acids: conventions and principles. *J. Biomol. Struct. Dyn.*, **6**, 655–667.
39. Zacharias,M. and Sklenar,H. (1999) Structural features of single-base bulgesin A-form DNA and RNA using a hierachical approach and energetic evaluation with a continuum solvent model. *J. Mol. Biol.*, **289**, 261–275.
40. Huang,S., Wang,Y. and Draper,D. (1996) Structure of a hexanucleotide RNA hairpin loop conserved in ribosomal RNAs. *J. Mol. Biol.*, **258**, 308–321.
41. Fountain,M.A., Serra,M.J., Krugh,T.R. and Turner,D.H. (1996) Structural features of a six-nucleotide RNA hairpin loop found in ribosomal RNA. *Biochemistry*, **35**, 6539–6548.
42. Kim,S.H., Suddath,F.L., Quigley,G.J., McPherson,A., Sussman,J.L., Wang,A.H., Seeman,N.C. and Rich,A. (1974) Three-dimensional tertiary structure of yeast phenylalanine tranfer RNA. *Science*, **185**, 435–440.
43. Durant,Ph.C., Bajji,A.C., Sundaram,M., Kumar,R.K. and Davis,D.R. (2005) Structural effects of hypermodified nucleosides in *E.coli* and Hyman tRNA^{lys} anticodon loop: the effect of nucleosides s^2U, mcm^5U, mcm^5s^2U, mnm^5s^2U, t^6A and ms^2t^6A. *Biochemistry*, **44**, 8078–8089.
44. Durant,Ph.C. and Davis,D.R. (1999) Stabilization of the anticodon stem–loop of tRNALys,3 by an A+-C base-pair and pseudouridine. *J. Mol. Biol.*, **265**, 115–131.
45. Sundaram,M., Durant,P. and Davis,D.R. (2000) Hypermodified nucleosides in the anticodon of lys-tRNA stabilize a canonical U-turn structure. *Biochemistry*, **39**, 12575–12584.
46. Bénas,P., Bec,G., Keith,G., Marquet,R., Ehresmann,C., Ehresmann,B. and Dumas,P. (2000) The crystal structure of HIV-reverse-transcription primer tRNA(lys,3) shows a canonical anticodon loop. *RNA*, **6**, 1347–1355.
47. von Ahsen,W., Green,R., Schroeder,R. and Noller,H.F. (1997) Identification of 2′-hydroxylgroups required for interaction of tRNA anticodon stem–loop region with the ribosome. *RNA*, **3**, 49–56.